

An Operational, Real-Time Forecasting System for 250 MW of PV Power Using NWP, Satellite, and DG Production data

William F. Holmgren¹, Antonio T. Lorenzo¹, Michael Leuthold², Chang Ki Kim², Alexander D. Cronin¹, and Eric A. Betterton²

1. University of Arizona, Department of Physics, Tucson, AZ, 85721, USA

2. University of Arizona, Department of Atmospheric Sciences, Tucson, AZ, 85721, USA

Abstract — We developed a real-time PV power forecasting system for Tucson Electric Power using a combination of high-resolution numerical weather prediction, satellite imagery, distributed generation (DG) production data, and irradiance sensors. The system provides forecasts with 10 second resolution for the first 30 minutes and 3 minute resolution out to 3 days. Forecasts out to 30 minutes are updated every 60 seconds based on new data from DG installations and irradiance sensors.

Index Terms — forecasting, real-time systems, sensors, solar energy.

I. INTRODUCTION

The need for PV power forecasting to support grid integration is well established [1-4]. We describe an operational hybrid forecasting system that utilizes input from 3 different sources: a high-resolution numerical weather prediction model, satellite imagery, and a network of distributed generation PV systems and irradiance sensors. Our forecasts are currently used at Tucson Electric Power to inform conventional generation resource allocation and to give system operators insight into behind-the-meter energy usage and generation. Our 10-second resolution short-term forecasts can help anticipate destabilizing ramp events, enable preemptive curtailment to avoid high ramp rates, and reduce the battery size needed to control ramp rates. Our long-term forecasts predict both solar and wind power production with 3-minute resolution, enabling day-ahead forecasts of the possibility of high variability. Integrating the forecasting technologies into a single hybrid forecast will improve the forecast accuracy at all time horizons and present end-users with a straightforward and simple product.

The field of solar power forecasting has quickly grown over the last several years. PV power forecasts have been made using numerical weather prediction [2, 5], satellite imagery [2, 6], total sky imagers [2, 7], and sensor networks [8]. The work we present here is, to our knowledge, the first work that combines a short-term forecasting method (i.e. total sky imagers or sensor networks) with both medium-term satellite imagery and long-term numerical weather modeling. We also emphasize that the work we present here represents the analysis of true forecasts, rather than retrospective modeling and analysis of historical data.

II. DATA SOURCES

In this section we provide a summary of the 3 different components of our forecasting system: a WRF numerical weather model, satellite imagery, and a network of DG PV systems and irradiance sensors.

A. Numerical Weather Prediction

The backbone of our forecast is a suite of high-resolution Weather Research and Forecasting (WRF) mesoscale numerical weather models. Each day we run four different models initialized using the 6Z and 12Z GFS and NAM forecasts, plus one additional forecast using cloud assimilation from satellite imagery. The models use a 5.4 km outer domain spanning 28.5° longitude by 20.75° latitude, and a 1.8 km inner domain spanning 7.7° longitude by 5.3° latitude. The consistency, or lack thereof, of the multiple model runs provides one estimate of the uncertainty of the WRF forecasts. We typically run the 6Z forecasts out to 72 hours and the 12Z forecasts out to 48 hours. Variables directly relevant to renewable power forecasting, including GHI, DNI, 10 meter winds, 80 meter winds, and 2 meter temperature, are output every 3 minutes. Figure 1 shows WRF forecasts for a 25 MW single-axis tracker installation.

The high spatial and temporal resolution of our WRF model enables direct prediction of local irradiance and variability, rather than relying on historical correlations between irradiance, variability and other model outputs. The high spatial resolution is also essential for accurate weather and irradiance modeling in regions with rapidly changing topography and land use, such as southern Arizona.

We used the NREL SOLRMAP OASIS station at the University of Arizona [9] to compare the WRF model predictions of GHI to the measured GHI. Calculations of the daily average mean absolute error (MAE) and normalized MAE (NMAE) of the WRF model GHI predictions are shown in Table I and Table II. We only considered times of the day at which the solar altitude was greater than 10 degrees. The MAE shown here was calculated at 3-minute resolution and MAE statistics for hourly forecasts are approximately 25% smaller. Normalization was calculated with respect to the clear sky irradiance at each time bin. For this work, we restrict our analysis of the WRF model runs to the month of April so that we can more directly compare them to the network forecasting

method discussed below and in reference [10]. Figure 2 shows the distribution and averages of the MAE errors for all forecast times.

Our WRF models outperformed a clear sky forecast by approximately 20% on day 1, 10% on day 2, and 15% on day 3. The curious observation that the day 3 forecast error is smaller than the day 2 forecast error is explained by the fact that not all models successfully run on all days and that clear days are significantly easier to forecast than cloudy days. Coincidentally, clear sky conditions were overrepresented in the models that ran out to 3 days.

TABLE I
MEAN ABSOLUTE ERROR (W/M²) OF GHI FORECAST (3 MIN. BINS)

Day	6Z-NAM	6Z-GFS	6Z	12Z-NAM	12Z-GFS	12Z	Mean	Clear sky
1	65.3	61.1	63.3	63.1	59.1	61.1	63.2	84.6
2	79.8	73.4	77.0	70.5	68.0	69.3	73.9	84.6
3	70.2	70.0	70.1	--	--	--	70.1	84.6

TABLE II
NORMALIZED MEAN ABSOLUTE ERROR (W/M²) OF GHI FORECAST (3 MIN. BINS)

Day	6Z-NAM	6Z-GFS	6Z	12Z-NAM	12Z-GFS	12Z	Mean	Clear sky
1	.101	.091	.096	.097	.090	.094	.094	.125
2	.120	.110	.115	.106	.102	.104	.109	.125
3	.105	.105	.105	--	--	--	.105	.125

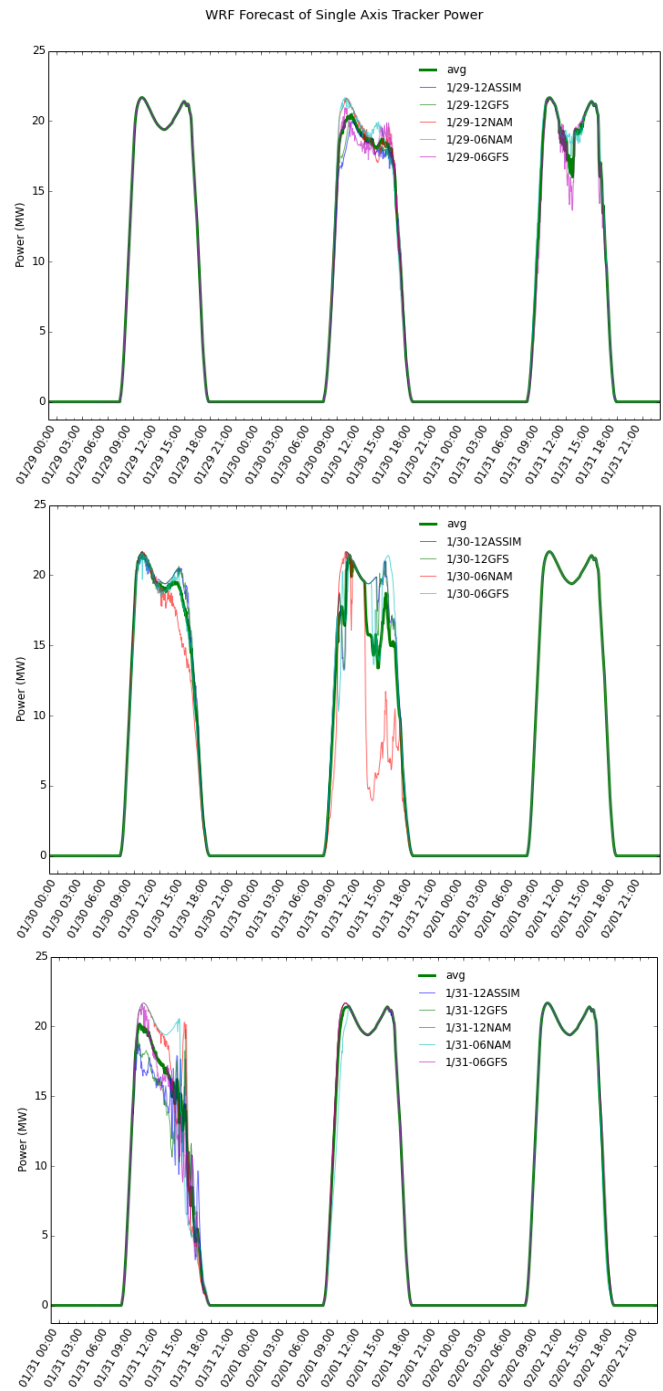


Fig. 1. WRF forecasts of single axis tracker PV power production for up to five different daily model runs (thin lines) and their averages (thick green). The top image shows model runs starting on January 29, 2014, the middle image shows models starting on January 30, and the bottom image shows models starting on January 31 so that one can observe how the forecast develops as new initialization data becomes available. The time axis is in MST. Figure 3 shows the satellite-derived irradiance on the variable afternoon of January 31.

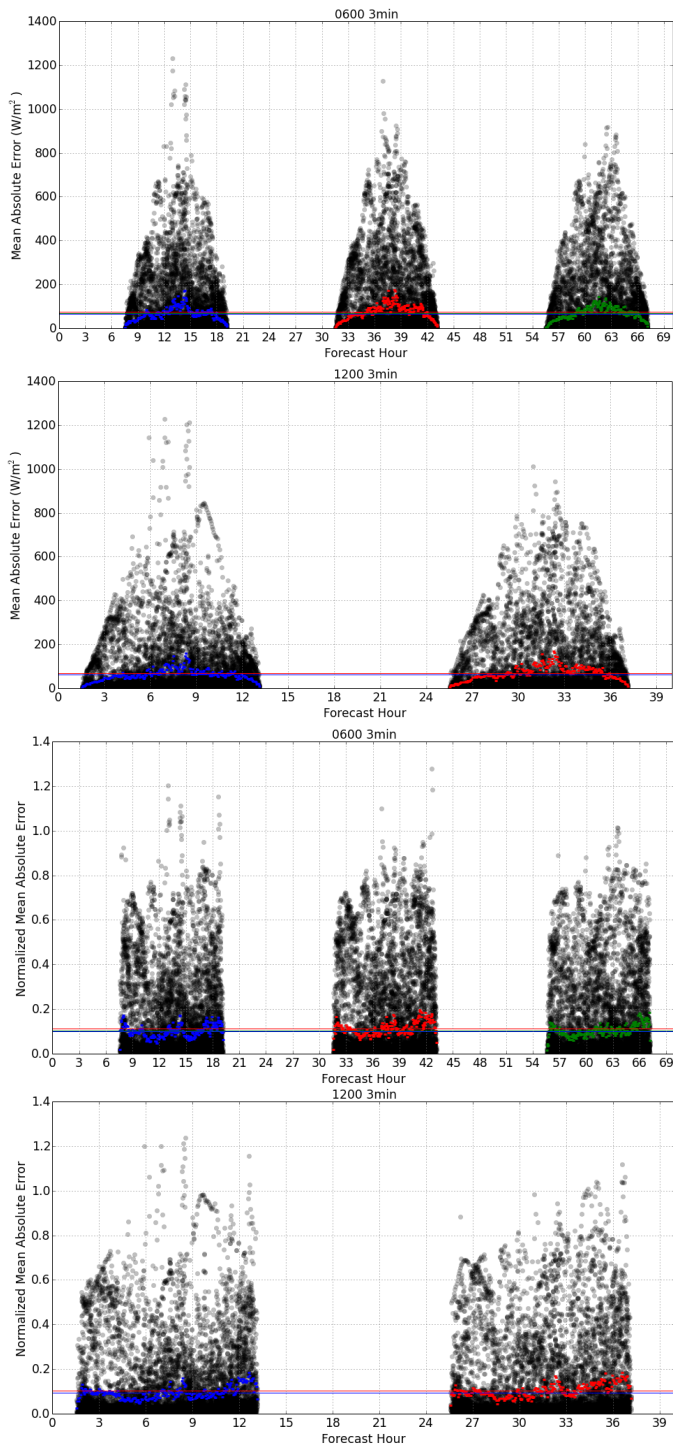


Fig. 2. GHI WRF forecast MAE and NMAE calculated every 3 minutes (grey dots) vs. forecast hour. Blue, red, and green dots show the average MAE at that forecast time across all 6Z or 12Z forecasts in the month of April, 2014. Blue, red, and green lines show the daily average MAE for days 1, 2, and 3, respectively. The data show a slight trend towards less accurate forecasts in the afternoons.

B. Satellite Imagery

Our WRF models, like all currently available numerical weather models, are insufficient to predict short-term variability with high confidence. The first method we use to predict short-term variability is satellite image processing. We use the visible and infrared channels of the GOES satellite imagery, combined with WRF model output, to determine the irradiance that reaches the ground. Figure 3 shows an example of the satellite derived irradiance map. The derived irradiance map can then be propagated forward in time using the WRF model wind speeds at the estimated cloud height. More sophisticated methods using image analysis algorithms do exist for satellite-based forecasting [2], however, we find that using the WRF model wind velocity is simple and still accurate for the majority of cloud systems in Southern Arizona. We will present a more detailed analysis of our satellite imagery forecasts in future work.

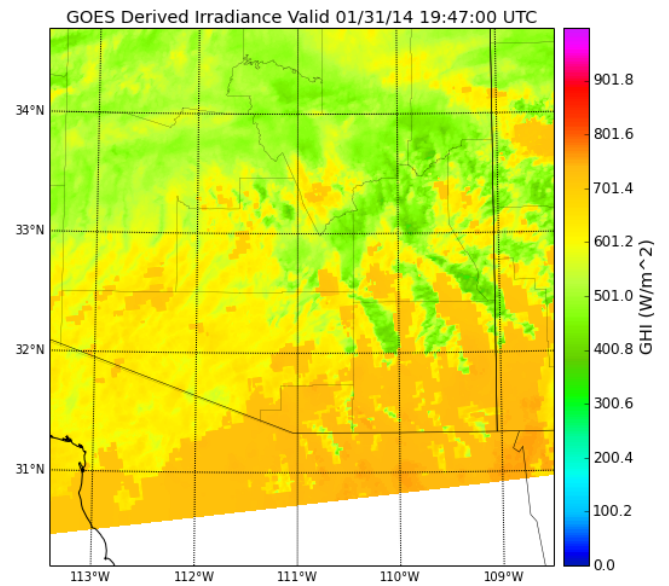


Fig. 3. GOES derived irradiance centered near Tucson, Arizona. This image corresponds to approximately 1/31 13:00 MST in Figure 1.

C. Network of irradiance sensors

A network of PV systems and irradiance sensors forms the final forecasting tool in our collection [8, 10]. We use PV output from 10 utility-scale systems and 20 residential systems as a proxy for irradiance. Data loggers on these systems send us data every 2 seconds to 15 minutes, depending on the system. We have also developed custom irradiance sensors that communicate via cellular modems. These sensors send us 1-second resolution data every 60 seconds. Figure 4 shows the network node locations and type.

The first step in creating a forecast from this sensor network is to create clear sky profiles for each sensor. We determine the sensor clear sky profiles using filtered historical data. We then interpret deviations from the clear sky profile as shadowing from clouds. We calculate the clearness index for

each sensor, and then calculate an interpolated clearness map across the forecasting domain. The WRF models' predicted wind velocities at cloud height determine the speed, direction, and uncertainty of the clearness map propagation in time. Finally, the forecasted PV power is determined from the propagated clearness map. For details, see [8, 10].

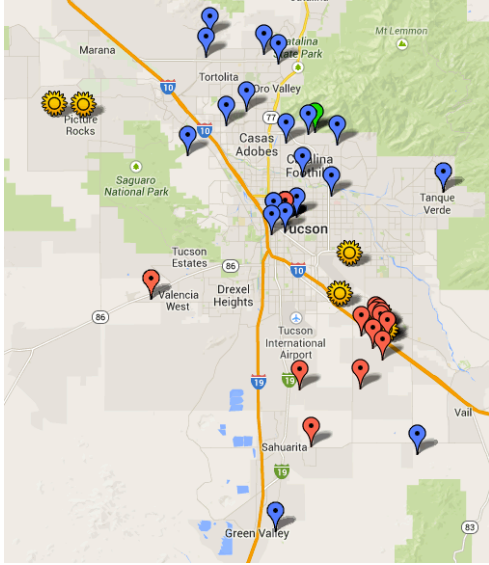


Fig. 4. Map of utility scale PV installations (suns), residential PV systems with data-monitoring hardware (blue and green pins), and custom-built irradiance sensors (red pins) used for PV power forecasting in the Tucson region.

III. HYBRID FORECASTING

We combine the WRF models, satellite imagery, and sensor network data into a single “hybrid forecast” for Tucson Electric Power. Figure 5 shows a comparison of the individual forecasts across 4 orders of magnitude in time. Network and persistence forecasts perform well for time scales shorter than 30 minutes, and WRF models perform best at longer time horizons. We anticipate that expanding the sensor network will enable it to outperform WRF forecasts out to 1-2 hours. Additional work is needed to evaluate our GOES satellite-based forecasts and combine them with the network and WRF forecasts.

The forecasts and their confidence intervals are automatically refreshed every minute throughout the day as new model runs, satellite images, or network data becomes available. We currently supply these forecasts to TEP via a website for 13 utility-scale PV power plants and an aggregate, shown in Figure 6. The data from our network of rooftop PV installations also informs an estimate of real-time behind-the-meter PV generation. We are working with TEP to integrate these forecasts into their Energy Management System.

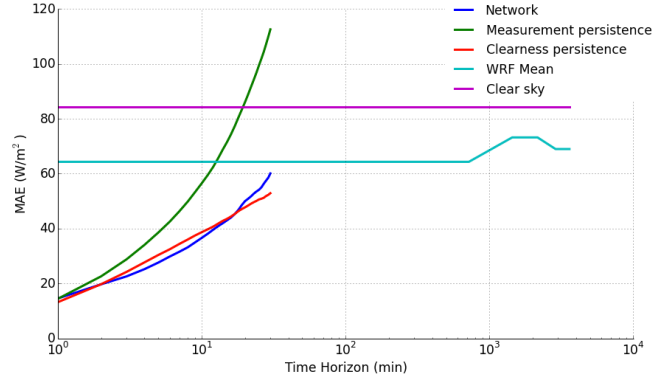


Fig. 5. Comparison of forecasted GHI MAE for 5 different forecasting techniques as a function of forecast time horizon. The WRF model forecast errors are daily averages.

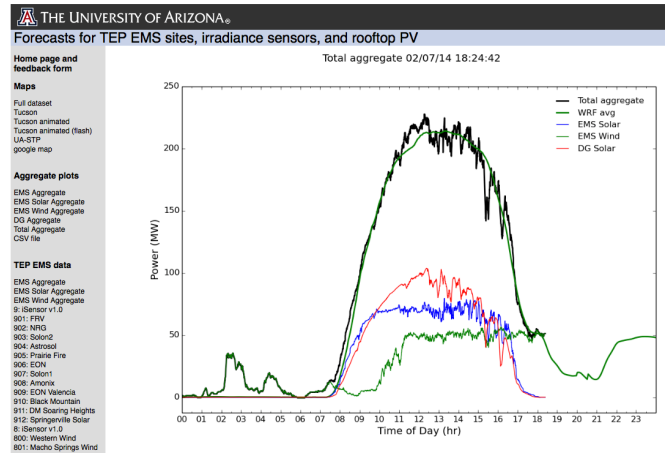


Fig. 6. Screenshot of website for delivering PV power forecasts to Tucson Electric Power. The day ahead forecasted total power production (thick green), measured utility scale solar (blue), measured distributed generation (red), and utility scale wind (thin green) is shown. Actual production is shown in black.

REFERENCES

- [1] D. Lew, G. Brinkman, E. Ibanez, A. Florita, M. Heaney, B.-M. Hodge, M. Hummon, G. Stark, J. King, S.A. Lefton, N. Kumar, D. Agan, G. Jordan, S. Venkataraman, “The Western Wind and Solar Integration Study Phase 2”, NREL, TP-5500-55588, 2013.
- [2] J. Kleissl, *Solar Energy Forecasting and Resource Assessment*. Oxford, UK: Elsevier, 2013.
- [3] S. Letendre, M. Makhyoun, and M. Taylor, *Predicting Solar Power Production: Irradiance Forecasting Models, Applications, and Future Prospects*. Washington, DC: SEPA, 2014.
- [4] R. Widdiss and K. Porter “A Review of Variable Generation Forecasting in the West,” NREL, SR-6A20-61035, 2014.
- [5] R. Perez, E. Lorenz, S. Pelland, M. Beauharnois, G.V. Knowe, K. Hemker, D. Heinemann, J. Remund, S.C. Muller, W. Traummuller, G. Steinmauer, D. Pozo, J.A. Ruiz-Arias, V. Lara-Fanego, L. Ramirez-Santigosa, M. Gaston-Romero, L.M.

- Pomares, "Comparison of numerical weather prediction solar irradiance forecasts in the US, Canada and Europe," *Solar Energy*, vol. 94, pp. 305-326, 2013.
- [6] J. Dise, A. Kankiewicz, J. Schlemmer, K. Hemker, S. Kivalov, T. Hoff, and R. Perez, "Operational Improvements in the Performance of the SUNY Satellite-to-Solar Irradiance Model Using Satellite Infrared Channels," in *39th IEEE Photovoltaic Specialist Conference*, 2013.
- [7] H. Yang, B. Kurtz, D. Nguyen, B. Urquhart, C. W. Chow, M. Ghonima, and J. Kleissl, "Solar irradiance forecasting using a ground-based sky imager developed at UC San Diego," *Solar Energy*, vol. 103, pp. 502-524, 2014.
- [8] V. Lonij, A. Brooks, A. Cronin, M. Leuthold, and K. Koch, "Intra-hour forecasts of solar power production using measurements from a network of irradiance sensors," *Solar Energy*, vol. 97, pp. 58-56, 2013.
- [9] NREL Solar Resource & Meteorological Assessment Project, Observed Atmospheric and Solar Information System. Data available online at <http://www.nrel.gov/midc/ua%5Foasis/>
- [10] A.T. Lorenzo, W.F. Holmgren, M. Leuthold, C.K. Kim, A.D. Cronin, and E.A. Betterton, "Short-term PV Power Forecasts Based on a Real-Time Irradiance Monitoring Network," in *40th IEEE Photovoltaic Specialist Conference*, 2014.